Structure−Activity Relationship and Mode of Action of N-(6-Ferrocenyl-2-naphthoyl) Dipeptide Ethyl Esters: Novel Organometallic Anticancer Compounds

Áine Mooney,[†,‡] Rachel Tiedt,[†,‡] Thamir Maghoub,[‡] Norma O'Donovan,[‡] John Crown,[‡,§] Blánaid White,[†] and Peter T. M. Kenny*,[†,‡]
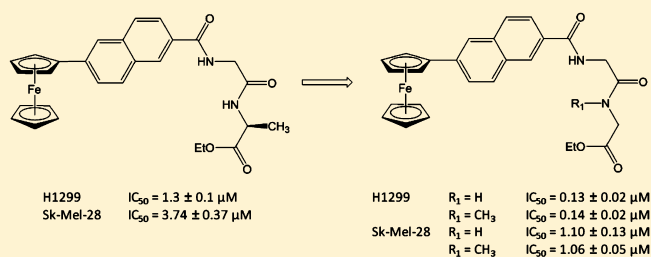
[†]School of Chemical Sciences, Dublin City University, Dublin 9, Ireland
[‡]National Institute for Cellular Biotechnology, Dublin City University, Dublin 9, Ireland
[§]Department of Medical Oncology, St. Vincent's University Hospital, Dublin 4, Ireland

S *Supporting Information*

ABSTRACT: In this article, we report the findings of a comprehensive structure−activity relationship study of N-(6-ferrocenyl-2-naphthoyl) dipeptide ethyl esters, in which novel analogues were designed, synthesized, and evaluated *in vitro* for antiproliferative effect. Two new compounds, **2** and **16**, showed potent nanomolar activity in the H1299 NSCLC cell line, with exceptional IC_{50} values of 0.13 and 0.14 μM, respectively. These compounds were also found to have significant activity in the Sk-Mel-28 malignant melanoma cell line (IC_{50} values of 1.10 and 1.06 μM, respectively). Studies were also conducted to elucidate the mode of action of these novel organometallic anticancer compounds. Cell cycle analysis in the H1299 cell line suggests these compounds induce apoptosis, while guanine oxidation studies confirm that **2** is capable of generating oxidative damage via a ROS-mediated mechanism.

H1299		IC_{50} = 1.3 ± 0.1 μM
Sk-Mel-28		IC_{50} = 3.74 ± 0.37 μM

H1299	R_1 = H	IC_{50} = 0.13 ± 0.02 μM
	R_1 = CH$_3$	IC_{50} = 0.14 ± 0.02 μM
Sk-Mel-28	R_1 = H	IC_{50} = 1.10 ± 0.13 μM
	R_1 = CH$_3$	IC_{50} = 1.06 ± 0.05 μM

INTRODUCTION

The medicinal application of ferrocene derivatives is currently a thriving area of research,[1] with applications in the area of cancer research being the most popular and well-researched.[2] To date, the most promising ferrocene-based drug candidates have been reported by Jaouen and co-workers;[3] these anticancer compounds contain a [3]-ferrocenophane motif and have a potent in vitro antiproliferative effect in breast and prostate cancer cells lines.

Our work is focused on developing a series of novel ferrocenyl-peptide bioconjugates that were found to exert a strong antiproliferative effect on the H1299 nonsmall cell lung cancer (NSCLC) cell line during preliminary in vitro studies.[4] These ferrocenyl-peptide bioconjugates are composed of three key moieties, namely, (i) an electroactive core, (ii) a conjugated aromatic linker, (iii) an amino acid or peptide derivative that can interact with other molecules via hydrogen bonds. One key feature of ferrocene is the ease by which it undergoes oxidation to form the ferricenium cation (Fc → Fc$^+$). This occurs in a reversible manner and is accommodated readily by the loss/gain of an electron from a nonbonding high energy molecular orbital. The redox properties of ferrocene have often been implicated in its cytotoxicity.[5] Indeed, ferricenium salts that are known to inhibit tumor growth have been shown to produce hydroxyl (HO$^•$) radicals under physiological conditions, leading to oxidatively damaged DNA.[6] In the case of our ferrocenyl-peptide bioconjugates, the presence of the conjugat-

ing aromatic linker between the ferrocene and peptide units lowers the redox potential to within the range of biologically accessible potentials, allowing for the interconversion between the ferrocene and ferricenium species. The catalytic generation of intracellular reactive oxygen species (ROS) such as the HO$^•$ radical offers an attractive and alternative method to target and kill cancer cells.[7]

In a previous study, we identified N-(6-ferrocenyl-2-naphthoyl)-glycine-L-alanine ethyl ester **1**, as a potential drug candidate since it has an in vitro antiproliferative effect that is comparable with cisplatin in the H1299 NSCLC cell line (IC_{50} value =1.3 ± 0.1 μM).[8] We have since conducted further studies in order to seek molecules that may have an even higher efficacy than **1**. Recently, we reported a study of N-(ferrocenyl)naphthoyl amino acid esters which found that N-(6-ferrocenyl-2-naphthoyl)-γ-aminobutyric acid ethyl ester was two times more potent than **1** in the H1299 NSCLC cell line (IC_{50} value =0.62 ± 0.07 μM).[9] This compound was also tested for in vitro antiproliferative activity in the Sk-Mel-28 malignant melanoma cell line and was found to have an encouraging IC_{50} value of 1.41 ± 0.04 μM. We herein report the results of a comprehensive structure−activity relationship (SAR) study of N-(6-ferrocenyl-2-naphthoyl) dipeptide ethyl esters that was conducted concomitantly. In addition, we report the results of

cell cycle analysis and guanine oxidation studies that were conducted to elucidate the mode of action of these novel organometallic anticancer compounds.

■ RESULTS AND DISCUSSION

Structure−Activity Relationship of 1. For our initial SAR study, we focused our attention on preparing a set of peptide chain analogues of **1** (Chart 1) to probe the steric and

Chart 1. N-(6-Ferrocenyl-2-naphthoyl)-glycine-L-alanine Ethyl Ester 1
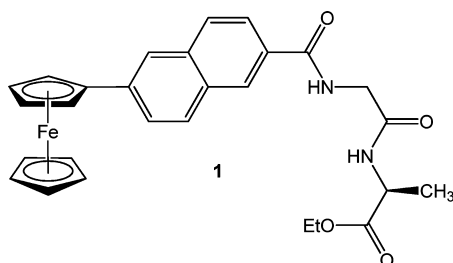
stereochemical requirements for potent antiproliferative activity. Previous studies of *N*-(ferrocenyl)benzoyl dipeptide derivatives had indicated that the in vitro antiproliferative effect is best when the small, neutral α-amino acids glycine and L-alanine are present in the peptide chain.[4c] However, the effect of the incorporation of α-amino acids with either branched alkyl or aromatic side chains into the dipeptide chain has yet to be investigated. A set of peptide chain analogues **2−8** containing either glycine or L-alanine as the first amino acid (aa) residue, and either glycine, L-alanine, L-leucine or L-phenylalanine as the second aa residue, were prepared by solution-phase peptide coupling of 6-ferrocenylnaphthalene-2-carboxylic acid to the appropriate free *N*-terminal dipeptide ethyl ester, using EDC/HOBt as the coupling reagent (Scheme 1). Inversion of the stereocenter of **1** was also investigated by preparing the inverse peptide chain analogue **9**. This was easily achieved by incorporating D-alanine as the second aa residue in the dipeptide chain **9a**, prior to solution-phase peptide coupling to 6-ferrocenylnaphthalene-2-carboxylic acid using EDC/HOBt (Scheme 2).

In Vitro Evaluation in the H1299 NSCLC Cell Line. The in vitro antiproliferative effect of the peptide chain analogues **2−9** was evaluated by performing a comprehensive screen at a single dose (10 μM) in the H1299 NSCLC cell line (Table 1).
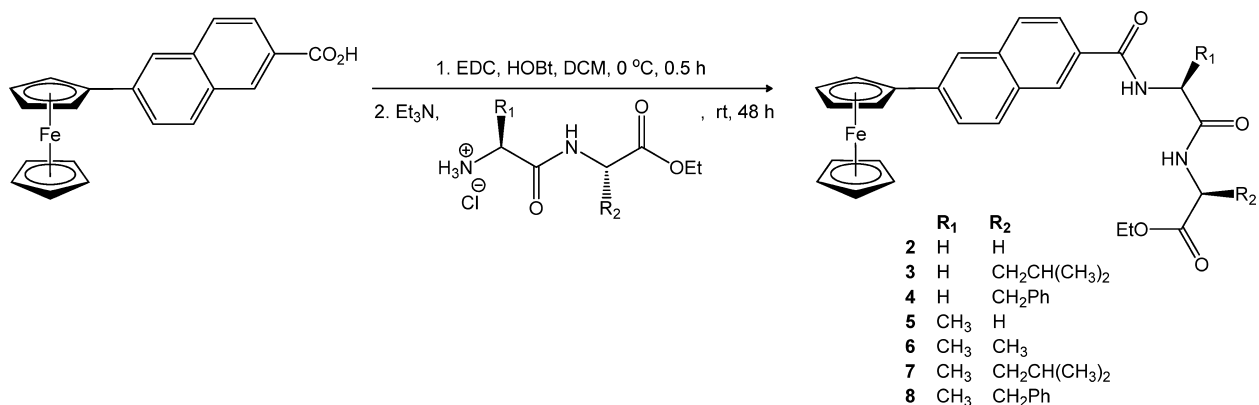
Compound **1** was also included in the screening to allow for the direct comparison of antiproliferative effect. At 10 μM, compounds **1−9** were all found to strongly inhibit cell proliferation in the H1299 cell line. The weakest antiproliferative effect was observed for **8**; however, this compound still achieved an appreciable level of cell growth inhibition (>50%). Four compounds in particular were shown to inhibit cell growth by almost 99%. Interestingly, none of these compounds contained either L-leucine or L-phenylalanine in the dipeptide chain. This indicates that although incorporation of bulkier amino acids is not completely detrimental to the antiproliferative effect, the presence of small, neutral aa residues glycine and L-alanine within the dipeptide chain is more favorable for biological activity.

Since compounds **1−9** were all found to inhibit cell growth by at least 50%, it was necessary to repeat the screening at the lower dose of 1 μM in order to identify the most potent derivatives. This second round of screening identified three compounds that inhibited cell growth by more than 50%: compounds **1** (∼70% growth inhibition), **2** (∼95% growth inhibition), and **9** (∼55% growth inhibition). IC$_{50}$ values were determined for analogues **2** and **9** in the H1299 cell line. The inverse peptide chain analogue **9** was found to be four times more potent than **1**, with an IC$_{50}$ value of 0.33 ± 0.02 μM. Thus, the in vitro antiproliferative activity of **1** was optimized by inverting the stereochemistry of the C-terminal α-carbon atom. This increase in antiproliferative effect may be a consequence of the increased resistance of **9** to degradation by proteases.[10]
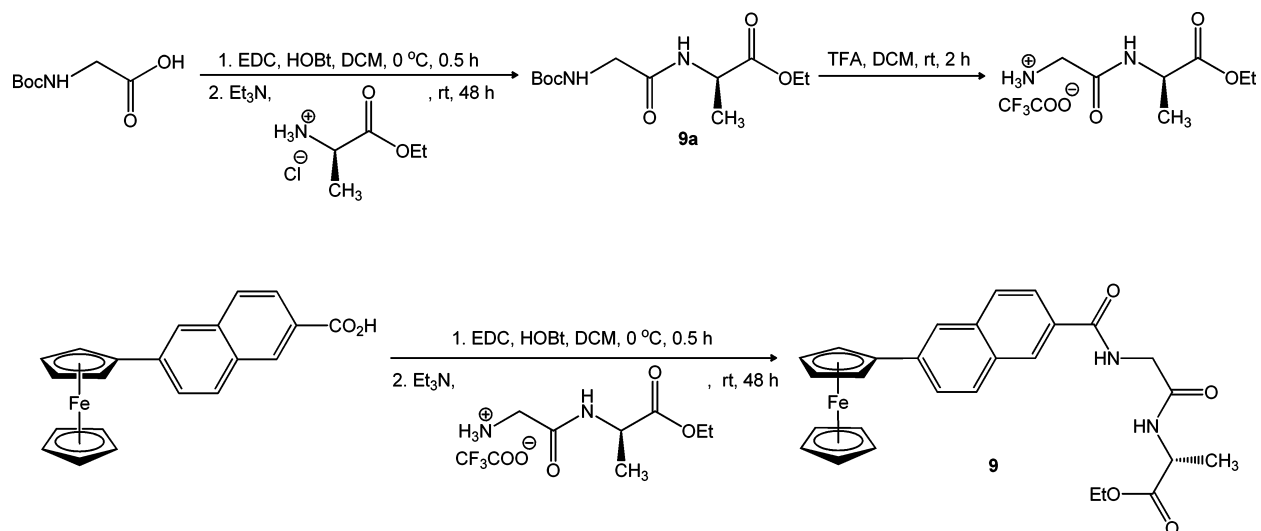
An exceptional IC$_{50}$ value of 0.13 ± 0.02 μM was calculated for **2**; the antiproliferative effect of this analogue is an order of magnitude greater than that of both cisplatin (IC$_{50}$ value of 1.5 ± 0.1 μM) and **1** in the H1299 cell line. Previous studies determined an IC$_{50}$ value of 20 μM for *N*-{ortho-(ferrocenyl)-benzoyl}-glycine−glycine ethyl ester in the same cell line.[4d] Thus, in this instance, over a 150-fold improvement in biological activity has been achieved by replacing the benzoyl linker with the naphthoyl linker. This is an extremely encouraging finding; there are only a number of other ferrocenyl compounds that have been reported recently in the literature to have comparable IC$_{50}$ values, and these derivatives have been tested in breast and prostate cancer cell lines.[3]

In Vitro Evaluation in Sk-Mel-28 Malignant Melanoma Cell Line. The in vitro antiproliferative effect of compounds **1−9** was also evaluated in the Sk-Mel-28 malignant melanoma

Scheme 1. Synthesis of Peptide Chain Analogues 2−8

	R$_1$	R$_2$
2	H	H
3	H	CH$_2$CH(CH$_3$)$_2$
4	H	CH$_2$Ph
5	CH$_3$	H
6	CH$_3$	CH$_3$
7	CH$_3$	CH$_2$CH(CH$_3$)$_2$
8	CH$_3$	CH$_2$Ph

Scheme 2. Synthesis of Inverse Peptide Chain Analogue 9

Table 1. Percentage Cell Growth of H1299 Cells in Presence of Compounds 1–9 and IC$_{50}$ Values[a]

compd	R$_1$	1st aa	2nd aa	% cell growth at 10 μM	% cell growth at 1 μM	IC$_{50}$[b] (μM)
1	Fc[c]	Gly	L-Ala	0.4 ± 0.7	31.3 ± 12.1	1.3 ± 0.1[d]
2	Fc	Gly	Gly	0.5 ± 0.8	4.4 ± 0.9	0.13 ± 0.02
3	Fc	Gly	L-Leu	4.9 ± 0.9	103.2 ± 11.0	
4	Fc	Gly	L-Phe	16.2 ± 5.3	102.9 ± 22.2	
5	Fc	L-Ala	Gly	0.4 ± 0.7	118.0 ± 9.1	7.8 ± 0.2[d]
6	Fc	L-Ala	L-Ala	0.1 ± 0.6	85.8 ± 5.7	3.7 ± 0.6[d]
7	Fc	L-Ala	L-Leu	13.0 ± 3.5	107.4 ± 16.1	
8	Fc	L-Ala	L-Phe	40.7 ± 8.0	98.8 ± 10.9	
9	Fc	Gly	D-Ala	1.9 ± 0.7	44.8 ± 3.0	0.33 ± 0.02
cisplatin						1.5 ± 0.1

[a]Mean of at least three independent experiments ± standard deviation. [b]IC$_{50}$ values were only determined for compounds having an antiproliferative effect, on H1299 at 1 μM, greater than 50%. [c]Fc = ferrocenyl (η^5-C$_5$H$_4$–Fe-C$_5$H$_5$). [d]Values are from ref 8.
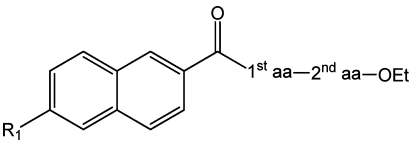
cell line at a single dose of 10 μM (Table 2). The Sk-Mel-28 cell line was found to be more resistant to treatment with 1–9 than the H1299 cell line. Only three compounds were found to inhibit cell growth by more than 50%: compounds 1 (~99% growth inhibition), 2 (~80% growth inhibition), and 9 (~85% growth inhibition). IC$_{50}$ values of 3.74 ± 0.37 μM, 1.10 ± 0.13 μM, and 1.83 ± 0.04 μM were calculated for compounds 1, 2, and 9, respectively. Although the antiproliferative effect of these compounds is not as strong in the Sk-Mel-28 cell line as in the H1299 cell line, these results are promising nonetheless since metastatic melanoma is notoriously resistant to chemotherapeutic drugs.[11]

Structure–Activity Relationship of 2. Considering the remarkable antiproliferative effect of 2, we decided to continue our SAR study by focusing on optimizing the biological activity of this compound. To determine if the unique chemistry of the redox active ferrocene unit was critical to the antiproliferative effect of 2, a nonorganometallic analogue 10 was prepared by solution-phase peptide coupling of 2-naphthoic acid to glycine–glycine ethyl ester hydrochloride, using EDC/HOBt (Scheme 3).

Previous studies of the N-(ferrocenyl)benzoyl peptide derivatives indicated that β-alanine and γ-aminobutyric acid could be of use as a potential isosteric replacement for glycine in the peptide chain.[12] For this reason, these two nonessential aa residues were incorporated into the dipeptide chain to yield a set of peptide chain analogues 11–14 (Chart 2).

Our final strategy was to prepare N-methylated derivatives of 2. This was achieved by incorporating the unusual aa sarcosine (N-methyl-glycine) into the dipeptide chain to yield the peptide chain analogues 15-17 (Chart 2). N-Methylation is a strategy widely used by scientists to alter pharmacological properties of peptides, such as metabolic stability, selectivity, potency, and bioavailability.[13] The inclusion of N-methyl amino acids within the dipeptide chain may also yield information concerning the importance of hydrogen bond formation for biological activity since the presence of an N-methyl group blocks the ability of the nitrogen atom to act as a hydrogen bond donor (HBD).

These unusual and nonessential aa residues were incorporated into compounds 11–17 by first of all preparing the Boc-protected dipeptide ethyl esters 11a–17a. This was achieved by

Table 2. Percentage Cell Growth of Sk-Mel-28 Cells in the Presence of Compounds 1−9 and IC$_{50}$ Values[a]

compd	R$_1$	1st aa	2nd aa	% cell growth at 10 μM	IC$_{50}$[b] (μM)
1	Fc[c]	Gly	L-Ala	0.7 ± 0.8	3.74 ± 0.37
2	Fc	Gly	Gly	19.0 ± 5.6	1.10 ± 0.13
3	Fc	Gly	L-Leu	79.0 ± 18.2	
4	Fc	Gly	L-Phe	95.4 ± 10.7	
5	Fc	L-Ala	Gly	74.7 ± 23.8	
6	Fc	L-Ala	L-Ala	55.9 ± 34	
7	Fc	L-Ala	L-Leu	86.3 ± 15.8	
8	Fc	L-Ala	L-Phe	102.6 ± 3.9	
9	Fc	Gly	D-Ala	15.6 ± 4.0	1.83 ± 0.04

[a]Mean of at least three independent experiments ± standard deviation. [b]IC$_{50}$ values were only determined for compounds having an antiproliferative effect, on Sk-Mel-28 at 10 μM, greater than 50%. [c]Fc = ferrocenyl (η^5-C$_5$H$_4$−Fe-C$_5$H$_5$).

solution-phase peptide coupling of the appropriate Boc-protected aa to the corresponding aa ethyl ester hydrochloride using EDC/HOBt (Scheme 4). Removal of the Boc-protecting groups from 11a−17a was achieved using an excess of trifluoroacetic acid in dichloromethane. The Boc-deprotected dipeptides were then coupled to 6-ferrocenylnaphthalene-2-carboxylic acid in the usual manner.

In Vitro Evaluation in H1299 and Sk-Mel-28 Cell Lines. The in vitro antiproliferative effect of compounds 10−17 was evaluated at a single dose of 1 μM in the H1299 cell line and 10 μM in the Sk-Mel-28 cell line (Table 3). Nonorganometallic analogue 10 did not exhibit an inhibitory effect on cell growth in either cell line. This dramatic loss of antiproliferative effect upon removal of the ferrocene unit from 2 demonstrates conclusively that this organometallic unit is essential for in vitro biological activity.

For the peptide chain analogues 11−14, compound 11 was the only derivative to exert an antiproliferative effect in the Sk-Mel-28 cell line (∼85% growth inhibition); however, this compound did not have any inhibitory effect on cell growth in the H1299 cell line. Compounds 12−14 failed to inhibit cell growth in either cell line. Thus, the isosteric replacement of the glycine residues in 2 with either β-alanine or γ-aminobutyric acid does not improve the in vitro biological activity.

In the case of the N-methylated analogues 15−17, compound 15 exhibited a strong antiproliferative effect in the Sk-Mel-28 cell line (∼97% growth inhibition) but did not have any effect on cell growth in the H1299 cell line. Compound 16, however, was shown to be a potent inhibitor of cell growth in both the H1299 (∼95% growth inhibition) and Sk-Mel-28

(∼85% growth inhibition) cell lines. Compound 17 failed to inhibit cell growth in either cell line. Thus, compound 16 was the only derivative for which IC$_{50}$ values were calculated: 0.14 ± 0.02 μM in the H1299 cell line and 1.06 ± 0.05 μM in the Sk-Mel-28 cell line. These IC$_{50}$ values are comparable with those determined for compound 2. Therefore, N-methylation of the first glycine residue does not alter the observed in vitro antiproliferative effect. This could prove to be a valuable modification for future studies since N-methyl derivatives are more resistant to degradation by proteases in vivo.[13] However, N-methylation of the second glycine residue results in a loss of potency in the H1299 cell line, while N-methylation of both residues produces a fall in antiproliferative effect in both cell lines. Thus, the ability of the nitrogen atom in the second glycine residue to act as a HBD is clearly important for biological activity.

Cell Cycle Analysis. Cell cycle analysis was performed on control samples and H1299 cells treated with the two most active compounds, 2 and 16, at concentrations of 0.5 μM and 1.0 μM (Figure 1). Table 4 summarizes the percentage of H1299 cells in each stage of the cell cycle following incubation with 2 for a period of 48 and 72 h. After 48 h, H1299 cells treated with 0.5 μM of 2 showed a significant increase in the sub-G0/G1 population (p = 0.006). There was also a significant decrease in the number of cells in the S phase of the cell cycle (p = 0.017). The sub-G0/G1 population was found to increase by approximately 2-fold when the concentration of 2 was increased to 1.0 μM. At this higher concentration, the increase in the sub-G0/G1 peak was accompanied by a concomitant decrease in the G0/G1 (p = 0.001) and S phase (p = 0.005) cell populations. Similar observations were made following incubation with 2 for 72 h; there was a significant increase in the sub-G0/G1 population of H1299 cells treated with 0.5 μM (p = 0.032) and 1.0 μM (p = 0.006) of 2.

The cell cycle distribution of H1299 cells incubated with 16 for a period of 48 and 72 h follows a similar pattern (Figure 2 and Table 5). After 48 h, there was a significant increase in the sub-G0/G1 population (p = 0.040) accompanied by a decrease in the number of cells in the S (p = 0.009) phase of the cell cycle, following treatment with the lower concentration (0.5 μM) of 16. Doubling the concentration of 16 to 1.0 μM also doubled the sub-G0/G1 population. At this higher concentration, there was also a significant decrease in the number of cells in the G0/G1 (p = 0.0004) and S (p = 0.002) phases of the cell cycle. After 72 h of incubation, there was a significant increase in the sub-G0/G1 population of H1299 cells treated with 0.5 μM (p = 0.012) and 1.0 μM (p = 0.015) of 16.

Thus, the exposure of H1299 cells to compounds 2 and 16 leads in both cases to an accumulation of hypodiploid cells (cells with a lower nuclear DNA content compared to that of normal diploid cells). These findings suggest that both compounds most likely induce apoptosis in H1299 cells since apoptotic cells are characterized by DNA fragmentation and

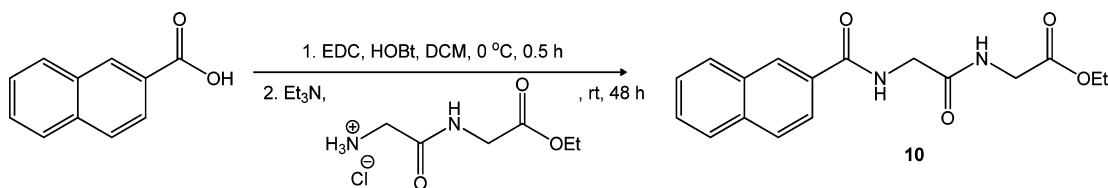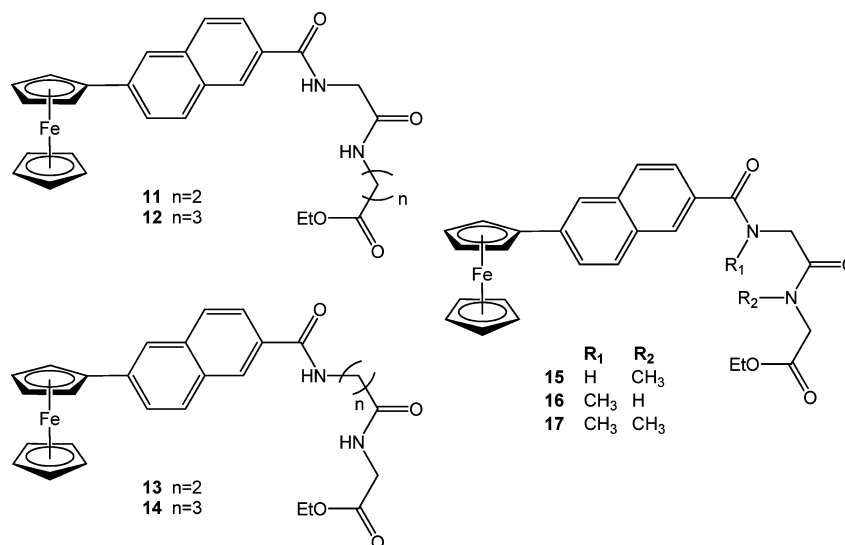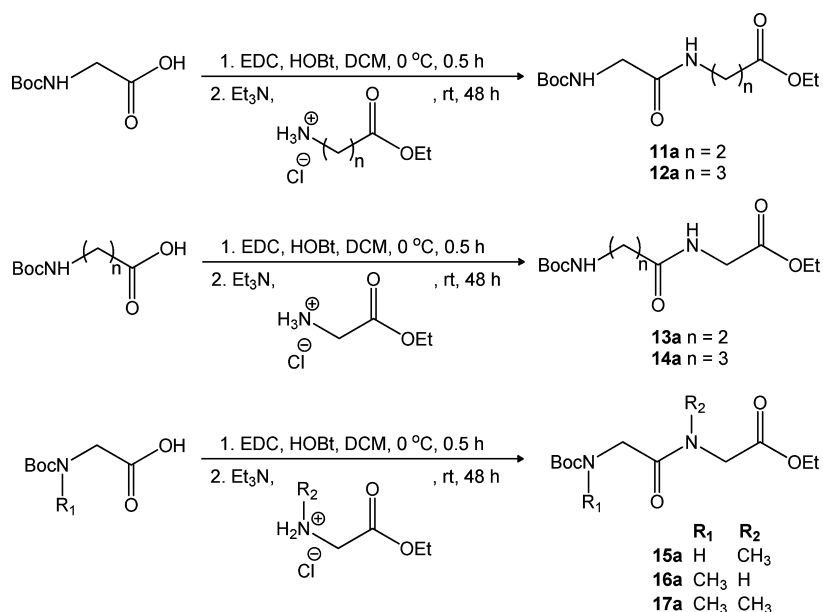**Scheme 3. Synthesis of Nonorganometallic Analogue 10**

Chart 2. Peptide Chain Analogues 11−17

11 n=2
12 n=3

13 n=2
14 n=3

	R_1	R_2
15	H	CH$_3$
16	CH$_3$	H
17	CH$_3$	CH$_3$

Scheme 4. Synthesis of Boc-Protected Dipeptide Ethyl Esters 11a−17a

11a n = 2
12a n = 3

13a n = 2
14a n = 3

	R_1	R_2
15a	H	CH$_3$
16a	CH$_3$	H
17a	CH$_3$	CH$_3$

consequently a decrease in nuclear DNA content. Similar observations have been made for the ferrocenyl derivative, ferrociphenol in the MCF-7 breast cancer cell line.[14] However, further flow cytometry studies that specifically measure the levels of early and late apoptotic cells would be required to confirm the induction of apoptosis by these novel compounds, as the presence of hypodiploid cells is not conclusive proof of apoptotic death.[15]

Guanine Oxidation Studies. A potential mechanism by which these novel organometallic anticancer compounds may induce DNA damage is by the catalytic generation of ROS. This is possible via a Fenton-type reaction, in which HO$^\bullet$ radicals are generated from the superoxide dismutation product, hydrogen peroxide (H$_2$O$_2$). To investigate this, the rate of Fenton reaction mediated 8-oxo-7,8-dihydroguanine (8-oxoGua)[16] formation from guanine was monitored. Guanine was chosen as it has the lowest oxidation potential of all the DNA bases and

is considered the clinical biomarker for oxidatively damaged DNA.[17]

The Fenton-mediated oxidation of guanine and the kinetic profile of 8-oxoGua formed as a result have previously been investigated using iron(II) sulfate (FeSO$_4$) and H$_2$O$_2$ to generate HO$^\bullet$ radicals.[18] To examine if compound **2** induces guanine oxidation via a similar mechanism, kinetic 8-oxoGua formation profiles were obtained by incubating free guanine with (i) FeSO$_4$ and H$_2$O$_2$ at 37 °C (Figure 3), and (ii) **2** and H$_2$O$_2$ at 37 °C (Figure 4). Samples were taken in duplicate over 15 min. Each sample was injected in triplicate and analyzed by HPLC-UV-EC using an electrochemical detector to detect 8-oxoGua at +550 mV versus Ag/AgCl. Control experiments were also carried out using either FeSO$_4$ or **2** in the absence of H$_2$O$_2$ and H$_2$O$_2$ in the absence of both iron compounds, to verify that any oxidation was Fenton-mediated. Additionally, they ensured that no artifactual oxidation was occurring from the sample preparation or analysis methodology.

Table 3. Percentage Cell Growth of H1299 and Sk-Mel-28 Cells in the Presence of Compounds 10−17 and IC$_{50}$ Values[a]

compd	R$_1$	1st aa	2nd aa	% cell growth at 1 μM in H1299	IC$_{50}$ (μM) in H1299	% cell growth at 10 μM in Sk-Mel-28	IC$_{50}$[b] (μM) in Sk-Mel-28
10	H	Gly	Gly	87.6 ± 18.4		95.6 ± 10.9	
11	Fc[c]	Gly	β-Ala	72.9 ± 5.2		14.8 ± 3.5	
13	Fc	Gly	GABA	97.5 ± 14.3		62.5 ± 30.7	
12	Fc	β-Ala	Gly	87.7 ± 8.1		98.4 ± 7.6	
14	Fc	GABA	Gly	102.8 ± 4.6		89.1 ± 17.8	
15	Fc	Gly	Sar	98.1 ± 4.4		3.2 ± 3.4	
16	Fc	Sar	Gly	4.8 ± 1.4	0.14 ± 0.02	15.7 ± 9.86	1.06 ± 0.05
17	Fc	Sar	Sar	102.2 ± 16.4		65.0 ± 29.8	
cisplatin					1.5 ± 0.1		

[a]Mean of at least three independent experiments ± standard deviation. [b]IC$_{50}$ values were only determined for compounds having an antiproliferative effect, on H1299 at 1 μM, greater than 50%. [c]Fc = ferrocenyl (η^5-C$_5$H$_4$−Fe-C$_5$H$_5$).
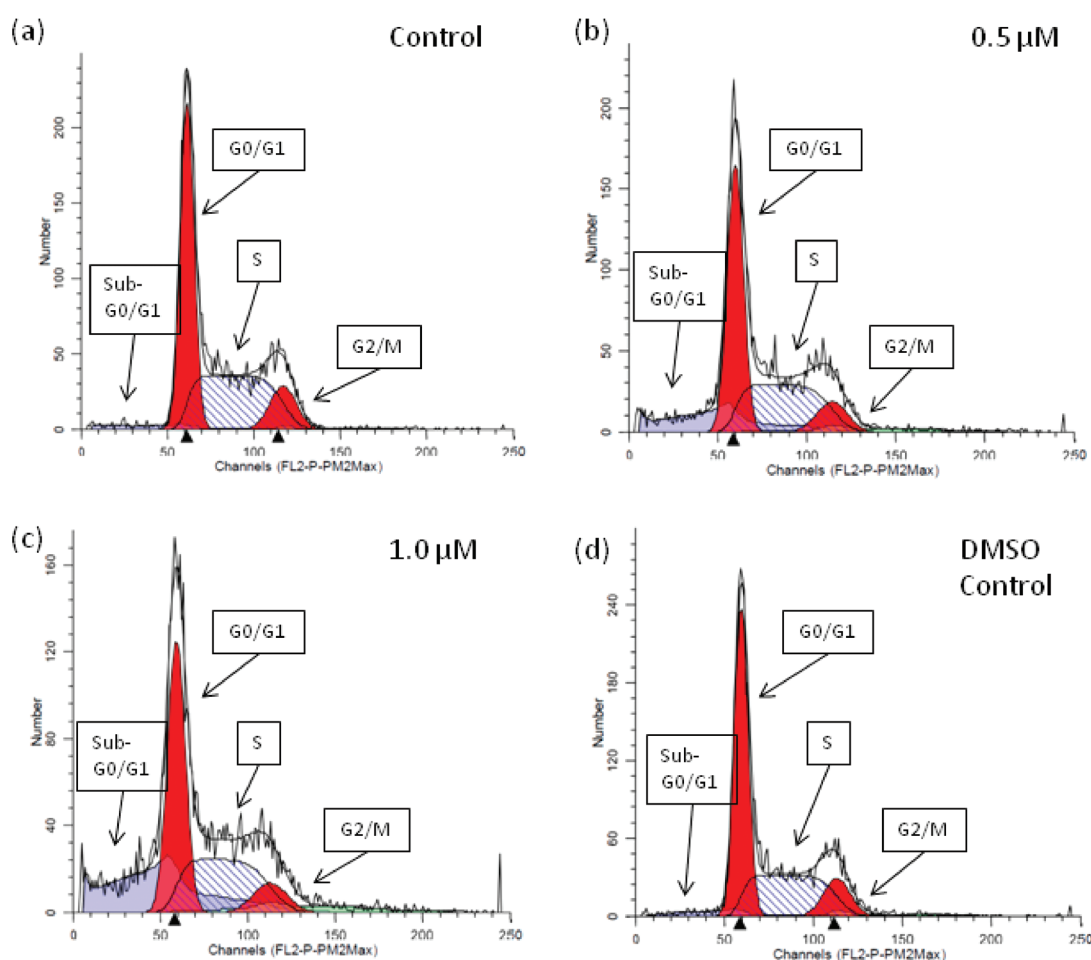

Figure 1. Sample graphs of H1299 cell cycle distribution after 72 h: (a) control, (b) 0.5 μM solution of 2, (c) 1.0 μM solution of 2, and (d) DMSO control. The data obtained from the flow cytometry was analyzed using ModFit software. This software calculates the number of diploid cells in G0/G1, S, and G2/M phases of the cell cycle, as well as cell debris and cell aggregates. Hypodiploid cells appear as a sub-G0/G1 peak.

Incubation of free guanine with (i) FeSO$_4$ and H$_2$O$_2$ led to oscillating concentrations of 8-oxoGua over the incubation period as previously reported.[18] The formation is significantly higher than the control baselines, confirming the oxidation is Fenton-mediated. The 8-oxoGua concentration maxima were 1.39 μM at 6 min and 2.29 μM at 8.5 min. This trend is analogous to that reported previously. These maxima occur with a different oscillation frequency, which can be attributed to differences in solution pH (previously, these maxima were reported at 4 and 15 min, respectively).

Table 4. Cell Cycle Distribution of H1299 Cells Incubated with 2 for 48 or 72 h, Then Analyzed by Flow Cytometry[a]

	sub G0/G1	G0/G1	S	G2/M
		48 h		
control	4.6 ± 1.1	40.9 ± 0.7	44.9 ± 1.8	9.6 ± 1.9
0.5 μM	11.9 ± 0.3**	39.6 ± 2.0	39.2 ± 0.8*	9.4 ± 1.4
1.0 μM	21.8 ± 1.6**	34.5 ± 0.8**	37.1 ± 1.2**	6.7 ± 1.4
DMSO control	5.3 ± 0.9	40.8 ± 0.9	44.4 ± 2.9	9.6 ± 1.3
		72 h		
control	2.4 ± 0.3	46.6 ± 0.4	41.3 ± 0.8	9.7 ± 1.2
0.5 μM	7.5 ± 1.7*	44.5 ± 2.0	39.2 ± 1.8	8.9 ± 2.0
1.0 μM	12.2 ± 1.5**	41.5 ± 3.1	37.9 ± 1.6*	8.4 ± 2.3
DMSO control	2.2 ± 0.4	47.9 ± 3.1	40.2 ± 3.6	9.7 ± 0.9

[a]Standard deviations have been calculated using data obtained from three independent experiments. Student's t-test was performed to determine significance: * denotes $p < 0.05$; ** denotes $p < 0.01$, when comparing treatment with the control or DMSO control.

Incubation of free guanine with (ii) **2** and H_2O_2, which was suspected to result in Fenton-mediated oxidation, also resulted in the formation of oscillating concentrations of 8-oxoGua over the incubation period. Again, the formation is significantly higher than the control baselines, clearly illustrating that both **2** and H_2O_2 are required to form this concentration of 8-oxoGua and confirming that the oxidation of guanine was Fenton-mediated. The maximum concentrations of 8-oxoGua formed with **2** were 0.62 μM after 30 s and 0.56 μM at 2 min. The concentration of 8-oxoGua generated by **2** is significantly lower than that generated by $FeSO_4$. Ferrocene may produce a weaker response than the $FeSO_4$ due to the presence of the cyclopentadienyl ligands and the size of the molecule. However, the generation of 8-oxoGua by **2** illustrates that the oxidation is occurring by Fenton chemistry and that **2** is generating oxidative damage via a ROS-mediated mechanism.

The oscillation period for 8-oxoGua formation mediated by **2** differs from that of $FeSO_4$. After the initial maxima at 0.5 and 2 min, the 8-oxoGua concentration continues to oscillate for the rest of the incubation period, with concentrations consistently higher than control levels, further confirming that oxidation is Fenton-mediated.

■ CONCLUSIONS

Our comprehensive structure–activity relationship study has shown that N-(6-ferrocenyl-2-naphthoyl) dipeptide ethyl esters are promising novel organometallic anticancer compounds. We have established the structural modifications that have a

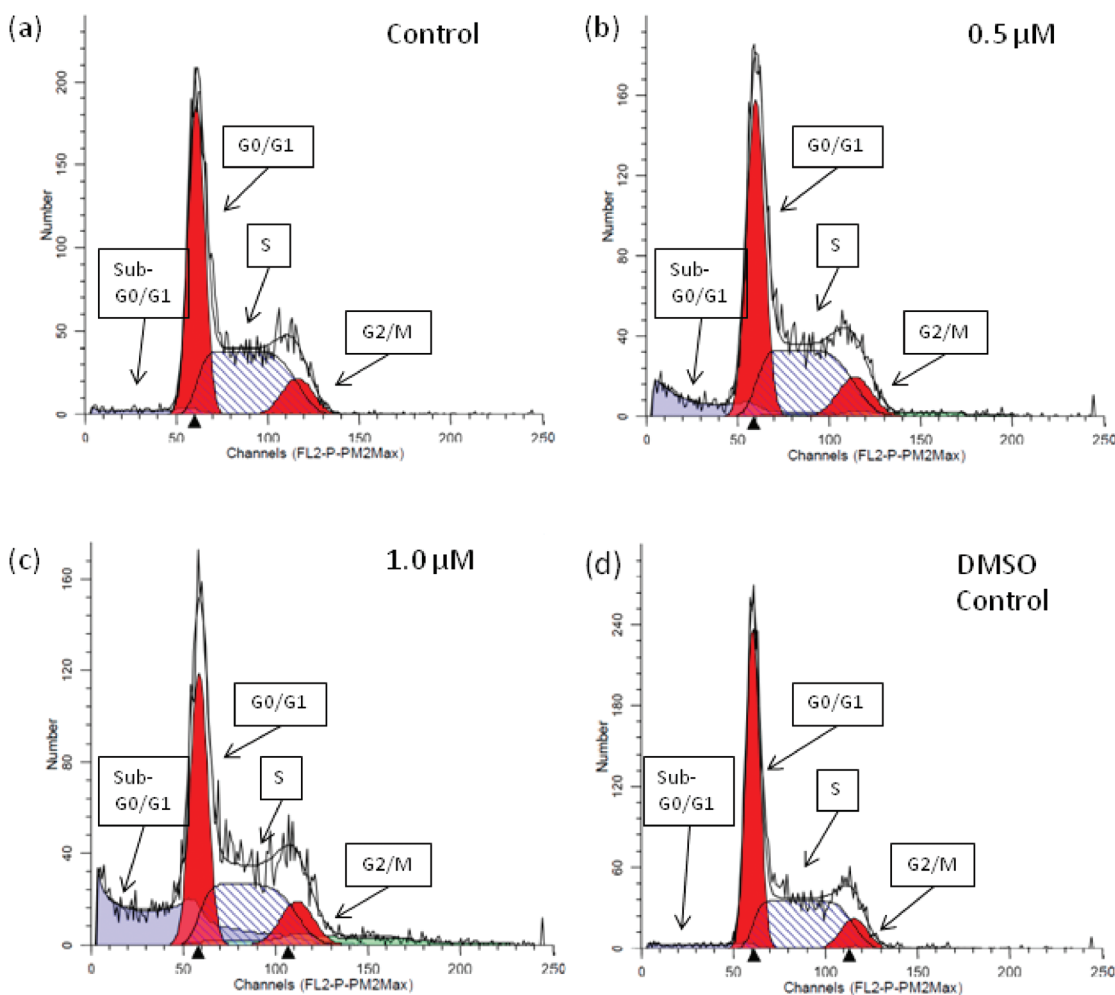**Figure 2.** Sample graphs of H1299 cell cycle distribution after 72 h: (a) control, (b) 0.5 μM solution of **16**, (c) 1.0 μM solution of **16**, and (d) DMSO control. The data obtained from flow cytometry was analyzed using ModFit software. This software calculates the number of diploid cells in G0/G1, S, and G2/M phases of the cell cycle, as well as cell debris and cell aggregates. Hypodiploid cells appear as a sub-G0/G1 peak.

Table 5. Cell Cycle Distribution of H1299 Cells Incubated with 16 for 48 or 72 h, Then Analyzed by Flow Cytometry[a]

	sub G0/G1	G0/G1	S	G2/M
		48 h		
control	3.6 ± 0.4	40.5 ± 0.6	46.4 ± 1.3	9.6 ± 1.0
0.5 μM	11.3 ± 2.8*	37.2 ± 2.0	41.3 ± 1.3**	10.2 ± 2.5
1.0 μM	19.5 ± 3.0**	34.0 ± 0.7**	38.9 ± 1.4**	7.6 ± 1.3
DMSO control	4.7 ± 1.0	39.8 ± 1.6	45.7 ± 2.9	9.8 ± 2.9
		72 h		
control	2.9 ± 0.2	42.4 ± 1.1	43.9 ± 0.1	10.8 ± 1.0
0.5 μM	6.0 ± 0.7*	41.1 ± 1.0	42.0 ± 1.0	10.8 ± 0.6
1.0 μM	11.3 ± 1.9*	38.4 ± 0.4*	40.3 ± 0.5**	10.1 ± 1.1
DMSO control	2.0 ± 0.4	44.0 ± 1.8	43.0 ± 0.7	11.0 ± 0.7

[a]Standard deviations have been calculated using data obtained from three independent experiments. Student's t-test was performed to determine significance: * denotes $p < 0.05$; ** denotes $p < 0.01$, when comparing treatment with the control.
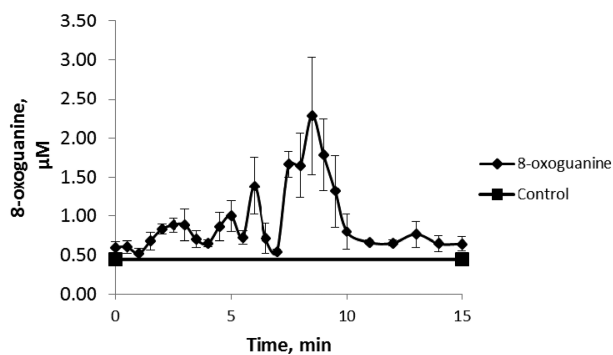

Figure 3. Concentration of 8-oxoGua formed as a function of time after the incubation of guanine with $FeSO_4$ and H_2O_2 at 37 °C. Error bars show the standard deviation of duplicate samples injected in triplicate.
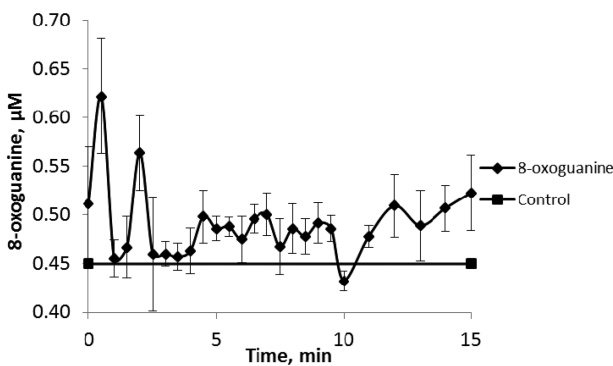

Figure 4. Concentration of 8-oxoGua formed as a function of time after the incubation of guanine with **2** and H_2O_2 at 37 °C. Error bars show the standard deviation of duplicate samples injected in triplicate.

positive impact and those that have a negative impact on the biological activity of these novel compounds. We have also clearly demonstrated that the organometallic ferrocene unit is essential for in vitro biological activity. Our study has identified two new compounds (**2** and **16**) that have a potent nanomolar activity in H1299 NSCLC cell line, with IC_{50} values of 0.13 and 0.14 μM, respectively. These compounds also have significant activity in the Sk-Mel-28 malignant melanoma cell line (IC_{50} values of 1.10 and 1.06 μM, respectively).

With regard to the proposed mode of action of these novel compounds, cell cycle analysis in the H1299 cell line has shown **2** and **16** to cause a significant increase in the sub-G0/G1 peak, which is suggestive of apoptosis. This observation is

encouraging since the production of intracellular ROS has been shown to lead to cancer cell apoptosis.[19]

Guanine oxidation studies confirm that **2** is capable of causing oxidative damage to guanine, and it does so by the generation of HO• radicals from H_2O_2. This finding is also consistent with the proposed mode of action. Further studies with ds-DNA are now required to demonstrate that **2** is capable of generating oxidatively damaged DNA. In addition, studies to detect the generation of intracellular ROS by these novel compounds are currently in progress.

■ EXPERIMENTAL SECTION

Chemistry. All chemicals were purchased from Sigma-Aldrich, Lennox Chemicals, Fluorochem Limited, or Tokyo Chemical Industry UK Limited, and used as received. Commercial grade reagents were used without further purification. When necessary, all solvents were purified and dried prior to use. Riedel-Haën silica gel was used for thin layer and column chromatography. Melting points were determined using a Stuart melting point (SMP3) apparatus and are uncorrected. Optical rotation measurements were made on a Perkin-Elmer 343 Polarimeter and are quoted in units of 10^{-1} deg cm^2 g^{-1}. Infrared spectra were recorded on a Perkin-Elmer Spectrum 100 FT-IR with ATR. UV–vis spectra were recorded on a Hewlett-Packard 8452 A diode array UV–vis spectrophotometer. ^1H and ^{13}C NMR spectra were recorded in deuterated solvents on either a Bruker Avance 400 NMR or a Bruker Avance Ultrashield 600 NMR. The ^1H and ^{13}C NMR chemical shifts are reported in ppm (parts per million). Tetramethylsilane (TMS) or the residual solvent peaks have been used as an internal reference. All coupling constants (J) are in Hertz. The abbreviations for the peak multiplicities are as follows: s (singlet), d (doublet), dd (doublet of doublets), t (triplet), q (quartet), qt (quintet), m (multiplet), and br (broad). Electrospray ionization mass spectra were performed on a Micromass LCT mass spectrometer or a Brüker Daltonics Esquire-LC ion trap mass spectrometer. Tandem mass spectra were obtained on a Micromass Quattro micro LC-MS/MS triple quadrupole mass spectrometer. Elemental analyses (C, H, N) of the target compounds, which were performed at the Microanalysis Laboratory at University College Dublin, are within 0.4% of the calculated values, confirming ≥95% purity. As reported previously for related compounds,[20] fractional moles of ethyl acetate and/or water could not be prevented despite 24−72 h of drying in vacuum.

Cyclic voltammograms were recorded in anhydrous acetonitrile (Sigma-Aldrich), with 0.1 M tetrabutylammonium perchlorate (TBAP) as a supporting electrolyte, using a CH Instruments 600a electrochemical analyzer (Pico-Amp Booster and Faraday Cage). The experiments were carried out at room temperature. A three-electrode cell consisting of a glassy carbon working electrode, a platinum wire counter electrode, and an Ag|AgCl reference electrode was used. The glassy carbon electrode was polished with 0.3 μm alumina followed by 0.05 μm alumina between each experiment to remove any surface

contaminants. The scan rate was 0.1 V s⁻¹. The concentration range of the ferrocene compounds was 1.0 mM in acetonitrile. The E^0 values obtained for the test samples were referenced relative to the ferrocene/ferricenium redox couple.

General Procedure for the Synthesis of *N*-(Ferrocenyl)-naphthoyl Dipeptide Ethyl Esters. 6-Ferrocenylnaphthalene-2-carboxylic acid was treated in DCM at 0 °C with 1.3 equiv of *N*-(3-dimethylaminopropyl)-*N*′-ethylcarbodiimide hydrochloride and 1.3 equiv of 1-hydroxybenzotriazole. After 30 min, an excess of triethylamine (5 mL) and 1 equiv of the corresponding dipeptide ethyl ester salt were added to the solution; the resulting mixture was raised to room temperature, and the reaction was allowed to proceed for 48 h. The reaction mixture was washed with water, and the DCM layer was then dried over MgSO₄. The solvent was removed in vacuo to give a residue that was then purified by silica gel column flash chromatography, eluting with a 1:1 mixture of hexane/ethyl acetate.

***N*-(6-Ferrocenyl-2-naphthoyl)-glycine−glycine Ethyl Ester 2.** Orange solid (0.33 g, 83%); mp 179−180 °C; E^0 47 mV vs Fc/Fc⁺. IR ν_{max} (KBr): 3407, 3340, 1732, 1654, 1650, 1558, 1494, 1213 cm⁻¹. UV−vis λ_{max} CH₃CN: 375 (ε 3485), 450 (ε 1497) nm. ¹H NMR (400 MHz, DMSO-d_6): 8.94 (1H, t, *J* = 5.6 Hz, −CON*H*-), 8.46 (1H, s, ArH), 8.38 (1H, t, *J* = 5.6 Hz, −CON*H*-), 8.06 (1H, s, ArH), 7.92−7.97 (3H, m, ArH), 7.82 (1H, dd, *J* = 1.6 and 8.4 Hz, ArH), 4.96 {2H, t, *J* = 1.6 Hz, *ortho* on (η^5-C₅H₄)}, 4.45 {2H, t, *J* = 1.6 Hz, *meta* on (η^5-C₅H₄)}, 4.10 (2H, q, *J* = 7.2 Hz, -OC*H₂*CH₃), 4.05 (5H, s, η^5-C₅H₅), 3.98 (2H, d, *J* = 5.6 Hz, -NHC*H₂*-), 3.87 (2H, d, *J* = 5.6 Hz, -NHC*H₂*-), 1.20 (3H, t, *J* = 7.2 Hz, -OCH₂C*H₃*); ¹³C NMR (100 MHz, DMSO-d_6): 169.8 (*C*=O), 169.6 (*C*=O), 166.5 (*C*=O), 138.8, 134.5, 130.6, 130.4, 128.7, 127.6, 127.3, 125.9, 124.6, 122.7, 84.0, 69.5, 69.4, 66.6, 60.4 (-ve DEPT), 42.5 (-ve DEPT), 40.7 (-ve DEPT), 14.0; HRMS (ESI⁺) *m/z* 499.1320 calcd. [M + H]⁺; found, 499.1296. Anal. (C₂₇H₂₆N₂O₄Fe) C, H, N.

***N*-(6-Ferrocenyl-2-naphthoyl)-glycine−L-leucine Ethyl Ester 3.** Orange solid (0.32 g, 58%); mp 160−161 °C; E^0 60 mV vs Fc/Fc⁺; $[\alpha]_D^{20}$ −12 (*c* 0.06 in CH₃CN); IR ν_{max} (neat) 3298, 2955, 1744, 1682, 1644, 1624, 1512, 1184 cm⁻¹. UV−vis λ_{max} (CH₃CN): 370 (ε 3336), 445 (ε 1422) nm. ¹H NMR (400 MHz, DMSO-d_6): 8.82 (1H, t, *J* = 5.6 Hz, −CON*H*-), 8.44 (1H, s, ArH), 8.34 (1H, d, *J* = 8.4 Hz, −CON*H*-), 8.06 (1H, s, ArH), 7.93−7.97 (3H, m, ArH), 7.82 (1H, dd, *J* = 1.2 and 8.4 Hz, ArH), 4.96 {2H, t, *J* = 2.0 Hz, *ortho* on (η^5-C₅H₄)}, 4.45 {2H, t, *J* = 2.0 Hz, *meta* on (η^5-C₅H₄)}, 4.30−4.35 (1H, m, -NHC*H*-), 4.07−4.13 (7H, m, -OC*H₂*CH₃, η^5-C₅H₅), 3.93−3.99 (2H, m, -NHC*H₂*-), 1.48−1.72 (3H, m, −C*H₂*C*H*-), 1.19 (3H, t, *J* = 7.2 Hz, -OCH₂C*H₃*), 0.86−0.92 {6H, m, −CH(C*H₃*)₂}. ¹³C NMR (100 MHz, DMSO-d_6): 172.5 (*C*=O), 169.1 (*C*=O), 166.5 (*C*=O), 138.8, 134.5, 130.7, 130.5, 128.7, 127.5, 127.3, 125.9, 124.5, 122.7, 84.1, 69.4, 66.6, 60.4 (-ve DEPT), 50.3, 42.2 (-ve DEPT), 40.1 (-ve DEPT), 24.2, 22.7, 21.4, 14.0; HRMS (ESI⁺) *m/z* 555.1946 calcd. [M + H]⁺; found, 555.1931. Anal. (C₃₁H₃₄N₂O₄Fe) C, H, N.

***N*-(6-Ferrocenyl-2-naphthoyl)-glycine−L-phenylalanine Ethyl Ester 4.** Orange solid (0.15 g, 56%); mp 53−54 °C; E^0 59 mV vs Fc/Fc⁺; $[\alpha]_D^{20}$ +18 (*c* 0.06 in CH₃CN); IR ν_{max} (neat) 3290, 3062, 1735, 1640, 1521, 1298, 1209 cm⁻¹. UV−vis λ_{max} (CH₃CN): 370 (ε 2894), 445 (ε 1242) nm. ¹H NMR (400 MHz, DMSO-d_6): 8.86 (1H, t, *J* = 5.6 Hz, −CON*H*-), 8.43−8.47 (2H, m, −CON*H*-, ArH), 8.10 (1H, s, ArH), 7.97−8.00 (3H, m, ArH), 7.86 (1H, dd, *J* = 1.2 and 8.4 Hz, ArH), 7.23−7.33 (5H, m, −CH₂*Ph*), 5.00 {2H, t, *J* = 1.6 Hz, *ortho* on (η^5-C₅H₄)}, 4.49−4.56 {3H, m, -NHC*H*-, *meta* on (η^5-C₅H₄)}, 3.93−4.10 (9H, m, -OC*H₂*CH₃, η^5-C₅H₅, -NHC*H₂*-), 2.98−3.13 (2H, m, −C*H₂*Ph), 1.15 (3H, t, *J* = 7.2 Hz, -OCH₂C*H₃*). ¹³C NMR (100 MHz, DMSO-d_6): 171.4 (*C*=O), 169.1 (*C*=O), 166.4 (*C*=O), 138.8, 136.9, 134.5, 130.7, 130.4, 129.1, 128.7, 128.2, 127.5, 127.3, 126.6, 125.9, 124.5, 122.7, 84.1, 69.4, 66.6, 60.5 (-ve DEPT), 53.7, 42.3 (-ve DEPT), 36.9 (-ve DEPT), 14.1; HRMS (ESI⁺) *m/z* 588.1711 calcd. [M]⁺•; found, 588.1693. Anal. (C₃₄H₃₂N₂O₄Fe·0.6C₄H₈O₂·0.15H₂O) C, H, N.

***N*-(6-Ferrocenyl-2-naphthoyl)-L-alanine−glycine Ethyl Ester 5.** See ref 8.

***N*-(6-Ferrocenyl-2-naphthoyl)-L-alanine−L-alanine Ethyl Ester 6.** See ref 8.

***N*-(6-Ferrocenyl-2-naphthoyl)-L-alanine−L-leucine Ethyl Ester 7.** Orange solid (0.10 g, 23%); mp 73−74 °C; E^0 60 mV vs. Fc/Fc⁺; $[\alpha]_D^{20}$ +29 (*c* 0.06 in CH₃CN); IR ν_{max} (neat) 3282, 3089, 1734, 1633, 1530, 1187 cm⁻¹. UV−vis λ_{max} (CH₃CN): 370 (ε 3064), 445 (ε 1298) nm. ¹H NMR (400 MHz, DMSO-d_6): 8.58 (1H, d, *J* = 7.2 Hz, −CON*H*-), 8.46 (1H, s, ArH), 8.29 (1H, d, *J* = 7.2 Hz, −CON*H*-), 8.05 (1H, s, ArH), 7.90−7.97 (3H, m, ArH), 7.79−7.86 (1H, m, ArH), 4.95 {2H, t, *J* = 1.6 Hz, *ortho* on (η^5-C₅H₄)}, 4.60 (1H, qt, *J* = 7.2 Hz, -NHC*H*-), 4.44 {2H, t, *J* = 1.6 Hz, *meta* on (η^5-C₅H₄)}, 4.26−4.32 (1H, m, -NHC*H*-), 4.00−4.14 (7H, m, -OC*H₂*CH₃, η^5-C₅H₅), 1.48−1.73 (3H, m, −C*H₂*C*H*-), 1.39 (3H, d, *J* = 7.2 Hz, −C*H₃*), 1.17 (3H, t, *J* = 7.2 Hz, -OCH₂C*H₃*), 0.86−0.93 {6H, m, −CH(C*H₃*)₂}. ¹³C NMR (100 MHz, DMSO-d_6): 172.7 (*C*=O), 172.4 (*C*=O), 166.0 (*C*=O), 138.7, 134.5, 130.6, 130.5, 128.7, 127.6, 127.2, 125.9, 124.7, 122.7, 84.1, 69.4, 66.6, 60.4 (-ve DEPT), 50.4, 48.6, 39.7 (-ve DEPT), 24.2, 22.7, 21.4, 17.9, 14.0; HRMS (ESI⁺) *m/z* 569.2103 calcd. [M + H]⁺; found, 569.2095. Anal. (C₃₂H₃₆N₂O₄Fe) C, H, N.

***N*-(6-Ferrocenyl-2-naphthoyl)-L-alanine−L-phenylalanine Ethyl Ester 8.** Orange solid (0.12 g, 23%); mp 75 °C; E^0 59 mV vs. Fc/Fc⁺; $[\alpha]_D^{20}$ +36 (*c* 0.06 in CH₃CN); IR ν_{max} (neat) 3282, 2963, 1736, 1634, 1526, 1260, 1187 cm⁻¹. UV−vis λ_{max} (CH₃CN): 370 (ε 2774), 445 (ε 1188) nm. ¹H NMR (400 MHz, DMSO-d_6): 8.58 (1H, d, *J* = 7.2 Hz, −CON*H*-), 8.45 (1H, s, ArH), 8.36 (1H, d, *J* = 7.2 Hz, −CON*H*-), 8.06 (1H, s, ArH), 7.93−7.97 (3H, m, ArH), 7.82 (1H, dd, *J* = 1.6 and 8.4 Hz, ArH), 7.17−7.25 (5H, m, −CH₂*Ph*), 4.96 {2H, t, *J* = 2.0 Hz, *ortho* on (η^5-C₅H₄)}, 4.60 (1H, qt, *J* = 7.2 Hz, -NHC*H*-), 4.43−4.50 {3H, m, -NHC*H*-, *meta* on (η^5-C₅H₄)}, 4.00−4.08 (7H, m, -OC*H₂*CH₃, η^5-C₅H₅), 2.96−3.07 (2H, m, −C*H₂*Ph), 1.36 (3H, d, *J* = 7.2 Hz, −C*H₃*), 1.10 (3H, t, *J* = 7.2 Hz, -OCH₂C*H₃*). ¹³C NMR (100 MHz, DMSO-d_6): 172.6 (*C*=O), 171.3 (*C*=O), 166.0 (*C*=O), 138.8, 137.0, 134.5, 130.6, 130.4, 128.7, 128.2, 127.6, 127.2, 126.5, 125.9, 124.7, 122.7, 84.1, 69.4, 66.6, 60.4 (-ve DEPT), 53.7, 48.6, 36.6 (-ve DEPT), 17.8, 14.1; HRMS (ESI⁺) *m/z* 602.1868 calcd. [M]⁺•; found, 602.1841. Anal. (C₃₅H₃₄N₂O₄Fe·0.45C₄H₈O₂) C, H, N.

***N*-(6-Ferrocenyl-2-naphthoyl)-glycine−D-alanine Ethyl Ester 9.** Orange solid (0.19 g, 41%); mp 73−74 °C; E^0 63 mV vs. Fc/Fc⁺; $[\alpha]_D^{20}$ +5 (*c* 0.05 in CH₃CN); IR ν_{max} (neat): 3290, 3084, 1733, 1640, 1529, 1450, 1206 cm⁻¹. UV−vis λ_{max} CH₃CN: 370 (ε 3048), 445 (ε 1288) nm. ¹H NMR (400 MHz, DMSO-d_6): 8.83 (1H, t, *J* = 5.6 Hz, −CON*H*-), 8.44 (1H, s, ArH), 8.39 (1H, d, *J* = 7.2 Hz, −CON*H*-), 8.06 (1H, s, ArH), 7.94−7.97 (3H, m, ArH), 7.83 (1H, dd, *J* = 1.6 and 8.4 Hz, ArH), 4.97 {2H, t, *J* = 2.0 Hz, *ortho* on (η^5-C₅H₄)}, 4.46 {2H, t, *J* = 2.0 Hz, *meta* on (η^5-C₅H₄)}, 4.31 (1H, qt, *J* = 7.2 Hz, -NHC*H*-), 3.91−4.14 (9H, m, -OC*H₂*CH₃, η^5-C₅H₅, -NHC*H₂*-), 1.31 (3H, d, *J* = 7.2 Hz, −C*H₃*), 1.20 (3H, t, *J* = 7.2 Hz, -OCH₂C*H₃*). ¹³C NMR (100 MHz, DMSO-d_6): 172.5 (*C*=O), 168.9 (*C*=O), 166.4 (*C*=O), 138.8, 134.5, 130.7, 130.5, 128.7, 127.5, 127.3, 125.9, 124.5, 122.7, 84.1, 69.4, 66.6, 60.4 (-ve DEPT), 47.7, 42.2 (-ve DEPT), 17.1, 14.0; HRMS (ESI⁺) *m/z* 512.1398 calcd. [M]⁺•; found, 512.1397. Anal. (C₂₈H₂₈N₂O₄Fe·0.45C₄H₈O₂) C, H, N.

***N*-(2-Naphthoyl)-glycine−glycine Ethyl Ester 10.** 2-Naphthoic acid (0.18 g, 1.0 mmol) was treated in DCM at 0 °C with *N*-(3-dimethylaminopropyl)-*N*′-ethylcarbodiimide hydrochloride (0.25 g, 1.3 mmol) and 1-hydroxybenzotriazole (0.18 g, 1.3 mmol). After 30 min, an excess of triethylamine (5 mL) and glycine−glycine ethyl ester hydrochloride (0.20 g, 1.0 mmol) was added to the solution; the resulting mixture was raised to room temperature, and the reaction was allowed to proceed for 48 h. The reaction mixture was washed with water, and the DCM layer was then dried over MgSO₄. The solvent was removed in vacuo to give a residue that was then purified by silica gel flash chromatography, eluting with a 1:1 mixture of hexane/ethyl acetate. The title compound was obtained as a white solid (0.28 g, 89%); mp 128−129 °C; IR ν_{max} (neat) 3264, 3056, 1738, 1646, 1633, 1619, 1546, 1203 cm⁻¹. ¹H NMR (400 MHz, DMSO-d_6): 9.05 (1H, t, *J* = 5.6 Hz, −CON*H*-), 8.58 (1H, s, -ArH), 8.46 (1H, t, *J* = 5.6 Hz, −CON*H*-), 8.10−8.02 (4H, m, -ArH), 7.71−7.64 (2H, m, -ArH), 4.15 (2H, q, *J* = 7.2 Hz, -OC*H₂*CH₃), 4.04 (2H, d, *J* = 5.6 Hz, -NHC*H₂*-), 3.92 (2H, d, *J* = 5.6 Hz, -NHC*H₂*-), 1.25 (3H, t, *J* = 7.2 Hz, -OCH₂C*H₃*). ¹³C NMR (100 MHz, DMSO-d_6): 169.8 (*C*=O), 169.6

(C=O), 166.5 (C=O), 134.2, 132.1, 131.3, 128.8, 127.8, 127.7, 127.62, 127.59, 126.7, 124.2, 60.4 (-ve DEPT), 42.5 (-ve DEPT), 40.7 (-ve DEPT), 14.0; HRMS (ESI$^+$) m/z 315.1345 calcd. [M + H]$^+$; found, 315.1360. Anal. ($C_{17}H_{18}N_2O_4$) C, H, N.

N-(6-Ferrocenyl-2-naphthoyl)-glycine−β-alanine Ethyl Ester 11. Orange solid (0.20 g, 43%); mp 148−149 °C; E^0 61 mV vs. Fc/Fc$^+$. IR ν_{max} (neat): 3312, 3084, 1728, 1677, 1639, 1625, 1538, 1185 cm^{-1}. UV−vis λ_{max} CH$_3$CN: 370 (ε 3006), 450 (ε 1288) nm. ^{1}H NMR (400 MHz, acetone-d_6): 8.32 (1H, s, ArH) 8.01 (1H, t, J = 5.6 Hz, −CONH-), 7.93 (1H, s, ArH), 7.78−7.86 (3H, m, ArH), 7.71 (1H, dd, J = 1.6 and 8.4 Hz, ArH), 7.34 (1H, br. s, −CONH-), 4.79 {2H, t, J = 2.0 Hz, ortho on (η^5-C$_5$H$_4$)}, 4.30 {2H, t, J = 2.0 Hz, meta on (η^5-C$_5$H$_4$)}, 3.91−3.97 (9H, m, -OCH_2CH$_3$, η^5-C$_5$H$_5$, -NHCH_2-), 3.35 (2H, q, J = 6.8 Hz, −CH_2CH$_2$−), 2.40 (2H, t, J = 6.8 Hz, −CH$_2$CH_2-), 1.06 (3H, t, J = 7.2 Hz, -OCH$_2$CH_3). ^{13}C NMR (100 MHz, acetone-d_6): 172.2 (C=O), 169.9 (C=O), 167.7 (C=O), 140.3, 136.1, 132.2, 131.7, 129.7, 128.5, 128.4, 126.9, 125.3, 123.9, 85.4, 70.4, 70.3, 67.6, 60.8 (-ve DEPT), 44.1 (-ve DEPT), 35.9 (-ve DEPT), 34.9 (-ve DEPT), 14.5; HRMS (ESI$^+$) m/z 512.1398 calcd. [M]$^{+\bullet}$; found, 512.1410. Anal. ($C_{28}H_{28}N_2O_4Fe\cdot0.2C_4H_8O_2\cdot0.1H_2O$) C, H, N.

N-(6-Ferrocenyl-2-naphthoyl)-glycine−γ-aminobutyric Acid Ethyl Ester 12. Orange solid (0.18 g, 38%); mp 140−142 °C; E^0 65 mV vs. Fc/Fc$^+$. IR ν_{max} (neat): 3374, 3246, 3082, 1704, 1672, 1638, 1566, 1538 cm^{-1}. UV−vis λ_{max} CH$_3$CN: 375 (ε 3070), 450 (ε 1312) nm. ^{1}H NMR (400 MHz, acetone-d_6): 8.32 (1H, s, ArH), 8.01 (1H, t, J = 5.6 Hz, −CONH-), 7.94 (1H, s, ArH), 7.78−7.86 (3H, m, ArH), 7.71 (1H, dd, J = 1.6 and 8.4 Hz, ArH), 7.33 (1H, br. s, −CONH-), 4.78 {2H, t, J = 2.0 Hz, ortho on (η^5-C$_5$H$_4$)}, 4.30 {2H, t, J = 2.0 Hz, meta on (η^5-C$_5$H$_4$)}, 3.90−3.96 (9H, m, -OCH_2CH$_3$, η^5-C$_5$H$_5$, -NHCH_2-), 3.15 (2H, q, J = 6.8 Hz, −CH_2CH$_2$CH$_2$−), 2.22 (2H, t, J = 7.2 Hz, −CH$_2$CH$_2$CH_2−), 1.66 (2H, qt, J = 7.2 Hz, −CH$_2$CH_2CH$_2$−), 1.06 (3H, t, J = 7.2 Hz, -OCH$_2$CH_3). ^{13}C NMR (100 MHz, acetone-d_6): 173.5 (C=O), 169.8 (C=O), 167.7 (C=O), 140.3, 136.1, 132.2, 131.8, 129.7, 128.5, 128.4, 126.9, 125.4, 123.9, 85.4, 70.4, 70.3, 67.6, 60.6 (-ve DEPT), 44.1 (-ve DEPT), 39.1 (-ve DEPT), 32.0 (-ve DEPT), 25.8 (-ve DEPT), 14.5; HRMS (ESI$^+$) m/z 527.1633 calcd. [M + H]$^+$; found, 527.1622. Anal. ($C_{29}H_{30}N_2O_4Fe$) C, H, N.

N-(6-Ferrocenyl-2-naphthoyl)-β-alanine−glycine Ethyl Ester 13. Orange solid (0.16 g, 34%); mp 171−172 °C; E^0 60 mV vs. Fc/Fc$^+$; IR ν_{max} (neat) 3357, 3282, 3073, 1735, 1678, 1633, 1600, 1540, 1214 cm^{-1}. UV−vis λ_{max} CH$_3$CN: 370 (ε 2758), 450 (ε 1154) nm. ^{1}H NMR (400 MHz, acetone-d_6): 8.28 (1H, s, ArH), 7.92 (1H, s, ArH), 7.76−7.84 (4H, m, −CONH-, ArH), 7.69 (1H, dd, J = 1.6 and 8.8 Hz, ArH), 7.51 (1H, br. s, −CONH-), 4.78 {2H, t, J = 1.6 Hz, ortho on (η^5-C$_5$H$_4$)}, 4.29 {2H, t, J = 1.6 Hz, meta on (η^5-C$_5$H$_4$)}, 4.02 (2H, q, J = 7.2 Hz, -OCH_2CH$_3$), 3.92 (5H, s, η^5-C$_5$H$_5$), 3.84 (2H, d, J = 5.6 Hz, -NHCH_2-), 3.59 (2H, q, J = 6.4 Hz, −CH_2CH$_2$−), 2.47 (2H, t, J = 6.4 Hz, −CH$_2$CH_2-), 1.09 (3H, t, J = 7.2 Hz, -OCH$_2$CH_3). ^{13}C NMR (100 MHz, acetone-d_6): 172.4 (C=O), 170.8 (C=O), 167.3 (C=O), 140.0, 135.9, 132.4, 132.2, 129.6, 128.4, 128.1, 126.9, 125.4, 123.9, 85.5, 70.4, 70.3, 67.6, 61.4 (-ve DEPT), 41.7 (-ve DEPT), 37.2 (-ve DEPT), 36.3 (-ve DEPT), 14.5; HRMS (ESI$^+$) m/z 512.1398 calcd. [M]$^{+\bullet}$; found, 512.1384. Anal. ($C_{28}H_{28}N_2O_4Fe\cdot0.25C_4H_8O_2\cdot0.1H_2O$) C, H, N.

N-(6-Ferrocenyl-2-naphthoyl)-γ-aminobutyric Acid−Glycine Ethyl Ester 14. Orange solid (0.14 g, 27%); mp 150−151 °C; E^0 60 mV vs. Fc/Fc$^+$. IR ν_{max} (neat): 3256, 3081, 1750, 1656, 1634, 1622, 1575, 1551, 1201 cm^{-1}. UV−vis λ_{max} CH$_3$CN: 370 (ε 2700), 450 (ε 1112) nm. ^{1}H NMR (400 MHz, DMSO-d_6): 8.67 (1H, t, J = 5.6 Hz, −CONH-), 8.45 (1H, s, ArH), 8.38 (1H, t, J = 6.0 Hz, −CONH-), 8.11 (1H, s, ArH), 7.94−8.01 (3H, m, ArH), 7.87 (1H, dd, J = 1.6 and 8.4 Hz, ArH), 5.02 {2H, t, J = 2.0 Hz, ortho on (η^5-C$_5$H$_4$)}, 4.50 {2H, t, J = 2.0 Hz, meta on (η^5-C$_5$H$_4$)}, 4.08−4.17 (7H, m, -OCH_2CH$_3$, η^5-C$_5$H$_5$), 3.88 (2H, d, J = 5.6 Hz, -NHCH_2-), 3.37−3.42 (2H, m, −CH_2CH$_2$CH$_2$−), 2.30 (2H, t, J = 7.2 Hz, −CH$_2$CH$_2$CH_2-), 1.87 (2H, qt, J = 7.2 Hz, −CH$_2$CH_2CH$_2$−), 1.25 (3H, t, J = 7.2 Hz, -OCH$_2$CH_3). ^{13}C NMR (100 MHz, DMSO-d_6): 172.5 (C=O), 170.0 (C=O), 166.2 (C=O), 138.6, 134.4, 131.1, 130.7, 128.7, 127.3,

127.2, 125.9, 124.5, 122.7, 84.1, 69.4, 66.6, 60.3 (-ve DEPT), 40.6 (-ve DEPT), 39.0 (-ve DEPT), 32.7 (-ve DEPT), 25.3 (-ve DEPT), 14.0; HRMS (ESI$^+$) m/z 527.1633 calcd. [M + H]$^+$; found, 527.1611. Anal. ($C_{29}H_{30}N_2O_4Fe$) C, H, N.

N-(6-Ferrocenyl-2-naphthoyl)-glycine−sarcosine Ethyl Ester 15. Orange solid (0.20 g, 43%); mp 64−65 °C; E^0 63 mV vs. Fc/Fc$^+$. IR ν_{max} (neat): 3300, 2928, 1739, 1626, 1507, 1480, 1200 cm^{-1}. UV−vis λ_{max} CH$_3$CN: 370 (ε 2670), 450 (ε 1098) nm. ^{1}H NMR (400 MHz, DMSO-d_6): 8.72, 7.45−7.51 (1H, t, J = 5.6 Hz, m, −CONH-, rotamers), 8.44−8.48 (1H, m, ArH), 8.05−8.07 (1H, m, ArH), 7.81−7.98 (4H, m, ArH), 4.95−4.97 {2H, m, ortho on (η^5-C$_5$H$_4$), rotamers}, 4.44−4.46 {2H, m, meta on (η^5-C$_5$H$_4$), rotamers}, 3.96−4.36 (11H, m, -OCH_2CH$_3$, η^5-C$_5$H$_5$, Gly CH_2, Sar CH_2, rotamers), 3.12, 3.01, 2.88 (3H, s, br. s, s, Sar CH_3, rotamers), 1.18−1.26 (3H, m, -OCH$_2$CH_3, rotamers). ^{13}C NMR (100 MHz, DMSO-d_6): 171.2 (C=O), 169.2 (C=O), 166.4 (C=O), 138.8, 134.5, 133.4, 130.7, 128.7, 128.2, 127.4, 125.9, 124.4, 122.7, 84.1, 69.4, 66.6, 60.9 (-ve DEPT), 60.5 (-ve DEPT), 49.3 (-ve DEPT), 40.8 (-ve DEPT), 35.2, 34.5, 30.7, 14.0; HRMS (ESI$^+$) m/z 512.1398 calcd. [M]$^{+\bullet}$; found, 512.1398. Anal. ($C_{28}H_{28}N_2O_4Fe$) C, H, N.

N-(6-Ferrocenyl-2-naphthoyl)-sarcosine−glycine Ethyl Ester 16. Red solid (0.18 g, 35%); mp 66−67 °C; E^0 55 mV vs Fc/Fc$^+$. IR ν_{max} (neat): 3291, 2930, 1745, 1677, 1623, 1507, 1396, 1196 cm^{-1}. UV−vis λ_{max} CH$_3$CN: 370 (ε 2492), 450 (ε 988) nm. ^{1}H NMR (600 MHz, DMSO-d_6): 8.61, 8.53 (1H, 2xbr. s, −CONH-, rotamers), 8.11 (1H, s, ArH), 7.95−8.03 (3H, m, ArH), 7.87 (1H, d, J = 8.4 Hz, ArH), 7.54−7.58 (1H, m, ArH), 5.01 {2H, t, J = 1.8 Hz, ortho on (η^5-C$_5$H$_4$)}, 4.49−4.52 {2H, m, meta on (η^5-C$_5$H$_4$)}, 3.96−4.26 (11H, m, -OCH_2CH$_3$, η^5-C$_5$H$_5$, Gly CH_2, Sar CH_2, rotamers), 3.08 (3H, s, Sar CH_3), 1.27 (3H, t, J = 7.2 Hz, -OCH$_2$CH_3). ^{13}C NMR (150 MHz, DMSO-d_6): 171.1 (C=O), 169.7 (C=O), 168.6 (C=O), 138.2, 133.4, 132.4, 130.7, 128.3, 126.5, 125.9, 125.0, 124.8, 122.8, 84.1, 69.41, 69.38, 66.6, 60.5 (-ve DEPT), 59.7 (-ve DEPT), 53.9 (-ve DEPT), 49.7 (-ve DEPT), 40.7 (-ve DEPT), 39.3, 34.1, 14.1; HRMS (ESI$^+$) m/z 512.1398 calcd. [M]$^{+\bullet}$; found, 512.1399. Anal. ($C_{28}H_{28}N_2O_4Fe\cdot0.2C_4H_8O_2\cdot0.25H_2O$) C, H, N.

N-(6-Ferrocenyl-2-naphthoyl)-sarcosine−sarcosine Ethyl Ester 17. Orange solid (0.05 g, 12%); mp 68−69 °C; E^0 58 mV vs. Fc/Fc$^+$. IR ν_{max} (neat): 2926, 1739, 1663, 1626, 1479, 1394, 1198 cm^{-1}. UV−vis λ_{max} CH$_3$CN: 370 (ε 2106), 450 (ε 836) nm. ^{1}H NMR (600 MHz, DMSO-d_6): 8.08−8.11 (1H, m, ArH), 7.86−8.02 (4H, m, ArH), 7.54, 7.42−7.46 (1H, d, J = 8.4 Hz, m, ArH, rotamers), 5.01 {2H, s, ortho on (η^5-C$_5$H$_4$)}, 3.87−4.51 {13H, meta on (η^5-C$_5$H$_4$), -OCH_2CH$_3$, η^5-C$_5$H$_5$, Sar CH_2, Sar CH_2, rotamers}, 3.03−3.16 (3H, m, Sar CH_3, rotamers), 2.88−3.01 (3H, m, Sar CH_3, rotamers), 1.24−1.32, 1.00 (3H, m, s, J = 7.2 Hz, -OCH$_2$CH_3, rotamers). ^{13}C NMR (150 MHz, DMSO-d_6): 171.0 (C=O), 169.1 (C=O), 168.1 (C=O), 138.1, 133.4, 132.5, 130.7, 128.2, 127.5, 126.3, 125.9, 124.7, 122.8, 84.2, 69.40, 69.38, 66.6, 60.58 (-ve DEPT), 60.54 (-ve DEPT), 52.48 (-ve DEPT), 49.60 (-ve DEPT), 49.23 (-ve DEPT), 48.36 (-ve DEPT), 38.34, 35.19, 34.47, 34.35, 14.1; HRMS (ESI$^+$) m/z 526.1555 calcd. [M]$^{+\bullet}$; found, 526.1536. Anal. ($C_{29}H_{30}N_2O_4Fe\cdot0.5C_4H_8O_2$) C, H, N.

Biological Assays: Cell Lines. Sk-Mel-28 was obtained from the Department of Developmental Therapeutics, National Cancer Institute (NCI) and H1299 from the American Tissue Culture Centre (ATCC). Cell lines were grown in RPMI-1640 supplemented with 10% fetal calf serum (FCS) at 37 °C in a 5% CO$_2$ humidified chamber.

In Vitro Proliferation Assays. Cells in the exponential phase of growth were harvested by trypsinization, and a cell suspension of 1 × 10^4 cells/mL was prepared in fresh culture medium. The cell suspension (100 μL) was added to a flat bottom 96-well plate (Costar, 3599), plates were agitated gently in order to ensure even dispersion of cells over the surface of the wells, and then cells were incubated for an initial 24 h in a 37 °C, 5% CO$_2$ incubator to allow cell attachment to the wells. A 10 mM stock solution of a test sample was prepared in dimethyl sulfoxide; dilute solutions of the test sample were prepared at 2× final concentration by spiking the cell culture medium with a calculated amount of the stock solution. Then, 100 μL aliquot of each dilute solution was added to each well of the plate, the plate

was gently agitated, and then incubated at 37 °C, 5% CO₂ for 5–6 days, until cell confluency reached 80–90%. Assessment of cell survival in the presence of the compounds **1–17** was determined by the acid phosphatase assay.[21] The acid phosphatase assay is highly sensitive and is easier to perform than the neutral red assay as it involves fewer steps and fewer reagents. It is also more convenient than the MTT assay because of the inherent problem of removal of the medium from the insoluble crystals. The reproducibility between replicate wells is excellent in the acid phosphatase assay, and in many cases, it has been shown to be better than the neutral red assay and the MTT assay. The percentage cell growth in the presence of each compound was determined relative to the control cells. The concentration of compounds causing 50% growth inhibition (IC$_{50}$ of the compound) was determined using Calcusyn (Biosoft, UK).

Cell Cycle Assays. H1299 cells were plated at a density of 2.5×10^4 cells/well in 24-well plates, in RPMI-1640 media containing 10% FCS. After 24 h, the cells were treated with the test compound. Dimethyl sulfoxide (DMSO) control wells were included in each assay. After 48 and 72 h, the media was collected into microcentrifuge tubes, and the wells were washed with PBS, which was also collected. Cells were trypsinized and added to the media collected for each sample. The tubes were centrifuged at 300g for 5 min, and the media were aspirated. The cell pellets were resuspended in PBS, and each cell suspension was transferred to a well of a round bottomed 96 well plate. The plate was centrifuged at 450g for 5 min and the supernatant aspirated leaving approximately 20 μL in each well. The remaining volume was used to resuspend the cells, and 200 μL of ice cold 70% ethanol was added gradually to each well. The plates were then stored at 4 °C overnight. After fixing, the cells were stained according to the protocol for the Guava Cell Cycle assay. Cells were analyzed on Guava EasyCyte (Guava Technologies), and the data was analyzed using Modfit LT software (Verity).

Statistical Analysis. Analysis of the response to treatment was performed using Student's t-test (two-tailed with unequal variance), and p-value <0.05 was considered statistically significant.

Guanine Oxidation Studies: Chemicals. Guanine was purchased from Sigma-Aldrich. 8-Oxo-7,8-dihydroguanine was purchased from Cayman Chemicals. Deionized water was purified using an ELGA purelab ultrasystem to a specific resistance of greater than 18.2 MΩ cm. All other chemicals were of analytical grade and used without further purification. All buffers and HPLC mobile phases were filtered through a 47 mm, 0.45 μm polyvinylidine fluoride (PVDF) micropore filter (Sartorius Stedim Biotech) before use.

Oxidation of Guanine. Ten millimolar guanine prepared in 84% 50 mM ammonium acetate, 85 mM acetic acid buffer, and 16% 1 M NaOH were incubated with 1 mM iron(II) sulfate (FeSO₄·6H₂O) or 1 mM *N*-(6-ferrocenyl-2-naphthoyl)-glycine–glycine ethyl ester **2** and 0.5 M hydrogen peroxide (H₂O₂) at 37 °C with constant stirring. Aliquots of 100 μL were taken in duplicate at various incubation times. The reaction was quenched with 1 mL of cold ethanol. The solution was dried immediately under a stream of nitrogen gas. Samples were stored at −20 °C until further use. Prior to analysis they were redissolved in 1 mL of 84% 50 mM ammonium acetate, 85 mM acetic acid buffer, and 16% 1 M NaOH. Samples were injected in triplicate.

HPLC-UV-EC Analysis of 8-oxoGua Formation. For 8-oxoGua analysis, the HPLC System consisted of a Varian ProStar 230 solvent delivery module and a Varian ProStar 310 UV–vis detector. A Phenomenex Onyx Monolithic C18 reversed phase column (100 × 4.6 mm) with 1 cm guard column was used. The eluent comprised 1.2% acetonitrile (ACN) and 50 mM ammonium acetate and was adjusted to pH 4.6 with glacial acetic acid. It was run at a flow rate of 4 mL min⁻¹ with an injection volume of 20 μL. The column temperature was ambient, and 8-oxoGua formation was monitored using an electrochemical detector at a detection potential of +550 mV versus an Ag/AgCl reference electrode.

Controlled Experiments. Control incubations were performed with guanine to ensure that no artificial oxidation was caused by the reaction conditions. Each of the reagents was sequentially replaced with deionized water to ensure that none of them could generate

oxidative damage individually. The highest background reading for these controls is plotted as the baseline in Figures 3 and 4.

■ ASSOCIATED CONTENT

ⓢ Supporting Information
Preparation details and spectroscopic data of Boc-protected dipeptide ethyl esters **9a** and **11a–17a**; a table containing the elemental analysis data of the novel compounds **2–4** and **7-17**. This material is available free of charge via the Internet at http://pubs.acs.org.

■ AUTHOR INFORMATION

Corresponding Author
*School of Chemical Sciences, Dublin City University, Glasnevin, Dublin 9, Ireland. Phone: + 353 1 700 5689. Fax: + 353 1 700 5503. E-mail: peter.kenny@dcu.ie.

Notes
The authors declare no competing financial interest.

■ ABBREVIATIONS USED

8-oxoGua, 8-oxo-7,8-dihydroguanine; β-Ala, β-alanine; D-Ala, D-alanine; ds-DNA, double stranded DNA; EDC, N-(3-dimethylaminopropyl)-N′-ethylcarbodiimide hydrochloride; Et₃N, triethylamine; Fc, ferrocene; Fc⁺, ferricenium ion; FeSO₄, iron(II) sulfate; H₂O₂, hydrogen peroxide; HO•, hydroxyl radical; HOBt, 1-hydroxybenzotriazole; MgSO₄, magnesium sulfate; NSCLC, nonsmall cell lung cancer; Sar, sarcosine

■ REFERENCES

(1) Fouda, M. F. R.; Abd-Elzaher, M. M.; Abdelsamaia, R. A.; Labib, A. A. On the Medicinal Chemistry of Ferrocene. *Appl. Organomet. Chem.* **2007**, *21*, 613–625.

(2) (a) Gasser, G.; Ott, I.; Metzler-Nolte, N. Organometallic Anticancer Compounds. *J. Med. Chem.* **2011**, *54*, 3–25. (b) Ornelas, C. Application of Ferrocene and its Derivatives in Cancer Research. *New J. Chem.* **2011**, *35*, 1973–1985.

(3) (a) Plazuk, D.; Vessieres, A.; Hillard, E. A.; Buriez, O.; Labbe, E.; Pigeon, P.; Plamont, M. A.; Amatore, C.; Zakrzewski, J.; Jaouen, G. A [3]-Ferrocenophane Polyphenol Showing a Remarkable Antiprolifer-ative Activity on Breast and Prostate Cancer Cell Lines. *J. Med. Chem.* **2009**, *52*, 4964–4967. (b) Gormen, M.; Plazuk, D.; Pigeon, P.; Hillard, E. A.; Plamont, M.-A.; Top, S.; Vessières, A.; Jaouen, G. Comparative Toxicity of [3]-Ferrocenophane and Ferrocene Moieties on Breast Cancer Cells. *Tetrahedron Lett.* **2010**, *51*, 118–120. (c) Gormen, M.; Pigeon, P.; Top, S.; Vessieres, A.; Plamont, M.-A.; Hillard, E. A.; Jaouen, G. Facile Synthesis and Strong Antiproliferative Activity of Disubstituted Diphenylmethylidenyl-[3]-Ferrocenophanes on Breast and Prostate Cancer Cell Lines. *MedChemComm* **2010**, *1*, 149–151.

(4) (a) Goel, A.; Savage, D.; Alley, S. R.; Kelly, P. N.; O'Sullivan, D.; Mueller-Bunz, H.; Kenny, P. T. M. The Synthesis and Structural Characterization of Novel N-Meta-Ferrocenyl Benzoyl Dipeptide Esters: The X-ray Crystal Structure and *in vitro* Anticancer Activity of N-{Meta-Ferrocenyl)benzoyl}-L-Alanine-Glycine Ethyl Ester. *J. Organomet. Chem.* **2007**, *692*, 1292–1299. (b) Corry, A. J.; Goel, A.; Alley, S. R.; Kelly, P. N.; O'Sullivan, D.; Savage, D.; Kenny, P. T. M. N-ortho-Ferrocenyl Benzoyl Dipeptide Esters: Synthesis, Structural

Characterization and *in vitro* Anticancer Activity of *N*-{Ortho-(Ferrocenyl)benzoyl}-Glycine-L-Alanine Ethyl Ester and *N*-{Ortho-(Ferrocenyl)benzoyl}-L-Alanine-Glycine Ethyl Ester. *J. Organomet. Chem.* **2007**, *692*, 1405−1410. (c) Corry, A. J.; O'Donovan, N.; Mooney, Á.; O'Sullivan, D.; Rai, D. K.; Kenny, P. T. M. Synthesis, Structural Characterization, *in vitro* Anti-Proliferative Effect and Cell Cycle Analysis of *N*-(Ferrocenyl)benzoyl Dipeptide Esters. *J. Organomet. Chem.* **2009**, *694*, 880−885. (d) Corry, A. J.; Mooney, Á.; O'Sullivan, D.; Kenny, P. T. M. Synthesis, Characterization and *in vitro* Anticancer Activity of *N*-(Ferrocenyl)benzoyl Tri- and Tetrapeptide Esters. *Inorg. Chim. Acta* **2009**, *362*, 2957−2961.

(5) Neuse, E. W. Macromolecular Ferrocene Compounds as Cancer Drug Models. *J. Inorg. Organomet. Polym. Mater.* **2005**, *15*, 3−32.

(6) Tabbi, G.; Cassino, C.; Cavigiolio, G.; Colangelo, D.; Ghiglia, A.; Viano, I.; Osella, D. Water Stability and Cytotoxic Activity Relationship of a Series of Ferricenium Derivatives. ESR Insights on the Radical Production During the Degradation Process. *J. Med. Chem.* **2002**, *45*, 5786−5796.

(7) Trachootham, D.; Alexandre, J.; Huang, P. Targeting Cancer Cells by ROS-Mediated Mechanisms: a Radical Therapeutic Approach? *Nat. Rev. Drug Discovery* **2009**, *8*, 579−591.

(8) Mooney, Á.; Corry, A. J.; O'Sullivan, D.; Rai, D. K.; Kenny, P. T. M. The Synthesis, Structural Characterization and *in vitro* Anticancer Activity of Novel *N*-(3-Ferrocenyl-2-Naphthoyl) Dipeptide Ethyl Esters and Novel *N*-(6-Ferrocenyl-2-Naphthoyl) Dipeptide Ethyl Esters. *J. Organomet. Chem.* **2009**, *694*, 886−894.

(9) Mooney, Á.; Corry, A. J.; Ni Ruairc, C.; Mahgoub, T.; O'Sullivan, D.; O'Donovan, N.; Crown, J.; Varughese, S.; Draper, S. M.; Rai, D. K.; Kenny, P. T. M. Synthesis, Characterisation and Biological Evaluation of *N*-(Ferrocenyl)naphthoyl Amino Acid Esters as Anticancer Agents. *Dalton Trans.* **2010**, *39*, 8228−8239.

(10) Adessi, C.; Soto, C. Converting a Peptide into a Drug: Strategies to Improve Stability and Bioavailability. *Curr. Med. Chem.* **2002**, *9*, 963−978.

(11) Eustace, A. J.; Crown, J.; Clynes, M.; O'Donovan, N. Preclinical Evaluation of Dasatinib, a Potent Src Kinase Inhibitor, in Melanoma Cell Lines. *J. Transl. Med.* **2008**, *6*, 53−64.

(12) Corry, A. J. Novel Ferrocenyl Benzoyl Peptide Esters as Anticancer Agents and Ferrocenoyl Self-Assembled Monolayers as Anion Sensors. Ph.D. Thesis, Dublin City University, 2009.

(13) Grauer, A.; Konig, B. Peptidomimetics: A Versatile Route to Biologically Active Compounds. *Eur. J. Org. Chem.* **2009**, 5099−5111.

(14) Nguyen, A.; Marsaud, V.; Bouclier, C.; Top, S.; Vessieres, A.; Pigeon, P.; Gref, R.; Legrand, P.; Jaouen, G.; Renoir, J. M. Nanoparticles Loaded with Ferrocenyl Tamoxifen Derivatives for Breast Cancer Treatment. *Int. J. Pharm.* **2008**, *347*, 128−135.

(15) Riccardi, C.; Nicoletti, I. Analysis of Apoptosis by Propidium Iodide Staining and Flow Cytometry. *Nat. Protoc.* **2006**, *1*, 1458−1461.

(16) Cooke, M. S.; Loft, S.; Olinski, R.; Evans, M. D.; Bialkowski, K.; Wagner, J. R.; Dedon, P. C.; Moller, P.; Greenberg, M. M.; Cadet, J. Recommendations for Standardized Description of and Nomenclature Concerning Oxidatively Damaged Nucleobases in DNA. *Chem. Res. Toxicol.* **2010**, *23*, 705−707.

(17) (a) van Loon, B.; Markkanen, E.; Hubscher, U. Oxygen as a Friend and Enemy: How to Combat the Mutational Potential of 8-oxo-Guanine. *DNA Repair* **2010**, *9*, 604−616. (b) Peoples, M. C.; Karnes, H. T. Recent Developments in Analytical Methodology for 8-Hydroxy-2 ′-Deoxyguanosine and Related Compounds. *J. Chromatogr., B* **2005**, *827*, 5−15.

(18) White, B.; Smyth, M. R.; Stuart, J. D.; Rusling, J. F. Oscillating Formation of 8-oxoGuanine During DNA Oxidation. *J. Am. Chem. Soc.* **2003**, *125*, 6604−6605.

(19) Kirshner, J. R.; He, S. Q.; Balasubramanyam, V.; Kepros, J.; Yang, C. Y.; Zhang, M.; Du, Z. J.; Barsoum, J.; Bertin, J. Elesclomol Induces Cancer Cell Apoptosis Through Oxidative Stress. *Mol. Cancer Ther.* **2008**, *7*, 2319−2327.

(20) Goel, A.; Savage, D.; Alley, S. R.; Hogan, T.; Kelly, P. N.; Draper, S. M.; Fitchett, C. M.; Kenny, P. T. M. The Synthesis and Structural Characterization of *N*-Para-Ferrocenyl Benzoyl Dipeptide Esters: The X-ray Crystal Structure of *N*-{Para-(Ferrocenyl)benzoyl}-L-Alanine-Glycine Ethyl Ester. *J. Organomet. Chem.* **2006**, *691*, 4686−4693.

(21) Martin, A.; Clynes, M. Acid Phosphatase: Endpoint for in vitro Toxicity Tests. *In Vitro Cell. Dev. Biol.* **1991**, *27A*, 183−184.